Molecular docking, ADMET and DFT, investigation of the prostate cancer inhibition potential of *Cinnamomum zeylanicum*

Abstract

The prostate gland found in men helps in semen production. When the prostate gland enlarges out of control, it could lead to prostate cancer. *Cinnamomum zeylanicum* (CZ) is a flavouring plant that is used as spice in foods. The anti-prostate properties of *Cinnamomum zeylanicum* were studied by molecular docking method. The chemical constituents of the plant were extracted in chloroform, Fourier transform infrared spectroscopy (FTIR) and gas chromatography-mass spectroscopy (GC-MS) examinations were performed to investigate the chemical constituents present. Absorption, distribution, metabolism, elimination and toxicity (ADMET) Screening were done to predict the drug-like properties, pharmacokinetics, and pharmacodynamics parameters of the identified compounds. Molecular docking analysis was used to identify the compound with the lowest binding energy using methyltrienolone as the control drug. Density functional theory was used to identify the relationship between the structures of the compounds and their chemical reactivity. the ADMET result showed that two of the compounds were carcinogens while thirty of them are safe for human consumption. Copaene gave the lowest binding energy. The DFT results revealed that the compounds showed low energy gap between the LUMO and HOMO energies making the molecule more reactive towards the drug target. The results showed that Cinnamomum zeylanicum is a good drug lead candidate for prostate cancer inhibition.

Key words: *Cinnamomum zeylanicum*, molecular docking, cancer, prostate, methyltrienolone, Copaene , inhibition

UNDER PEER REVIEW

1. INTRODUCTION

The prostrate is a small gland found in men, it forms part of the reproductive system since it helps in the production of semen. It gets enlarged as one grows old. Prostate cancer begins when the prostate cells grow out of control, it is a disease that affects men especially after the age of 40 [1-2]. One in every four men is known to suffer from prostate enlargement. It is one of the most rampant malignancies diagnosed in men around the globe [3-4]. Normal increase and preservation of the prostate is based on androgen hormones which act through the androgen receptor. Stimulating the androgen receptor triggers the formation of prostate cancer. Lately,

interest has moved towards identifying dietary ingredients that could exert anti-carcinogenic effects on prostate cancer cells [5-6]. It has been shown that food materials containing flavonoids can constrain androgen receptors thereby inhibit the growth of prostate cancer cells [7-8].

Cinnamomum zeylanicum an indigenous tropical spice is found in every household used mainly for its flavoring purpose. It has some medicinal applications; it is a member of the Lauraceae family. It has been reported to have several health benefits [9] such as inhibition of cancer growth, blood sugar regulation, cholesterol reduction, anti-bacterial, anti-viral, anti-fungi, anti-oxidant and anti-inflammatory properties. [10-14].

Molecular docking is a procedure employed in drug discovery and formulation to identify the correct protein– ligand binding configurations. This method usually involves the binding of a molecule with the correct macromolecule and then tabulating the binding free energy for the ligand and receptor [15-18]

The present work tries to evaluate phytochemicals in Cinnamomum zeylanicum for their prostate cancer growth inhibiting activities.

2. MATERIALS AND METHODS

2.1 Preparation of the *Cinnamomum zeylanicum*.

The *Cinnamomum zeylanicum* used in this study was harvested from a local farm in Imo state, dried and ground to powdered form, dipped in chloroform to extract its chemical constituents, filtered, concentrated and sent for FTIR and GC-MS analysis.

2.2 Identification of Phytochemicals

The prepared plant material was submitted for Fourier transform infrared spectroscopy (FTIR) and gas-chromatography mass spectrophotometry (GC-MS) analysis to identify the phytochemicals present. The FTIR examination was performed with SHIMADZU Model no 84008 at the National research institute, Zaria Kaduna State Nigeria [19]. GC-MS examination was performed at the Amadu Bello university research laboratory using Agilent 19091S-433UI GCMS model with parameters HP-5ms Ultra Inert 0 °C—325 °C (350 °C): 30 m x 250 μm x 0.25, the phytochemicals were then identified from the GC-MS result by comparing with the National Institute of Standards and Technology (NIST) mass spectral library [20]

2.3 Ligand Preparation

Three-dimensional structure-data files (SDF) of the compounds identified in the GC-MS analysis were downloaded from PubChem online software, minimized using the PyRx virtual screening tool at universal force of step 200, converted to Auto Dock ligands (pdbqt) [21] and used in the docking process.

2.4 Identification and Preparation of Protein Molecular Target

UNDER PEER REVIEW

The three dimensional (3D) structure of the human androgen receptor molecular target with PBD identity (1e3g) was identified from literature [22-23] and downloaded from protein database (PDB). The target was prepared in discovery studio software by removing the crystallographic water particles and co-crystallized ligand and saved as protein data band file for use in the molecular docking analysis. Figure 1 shows the human androgen receptor molecular target with the active site amino acid residues

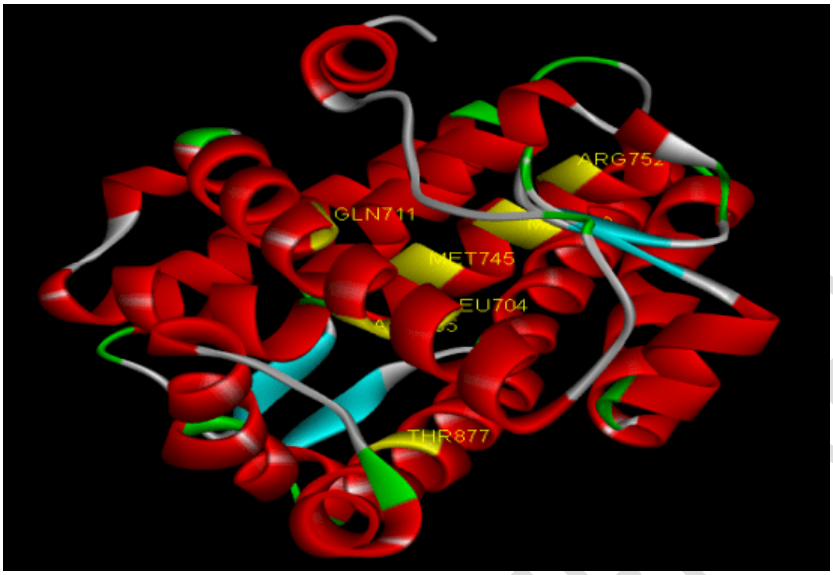

Figure 1. The human androgen receptor molecular target (PDB: 1e3g) with amino acid residues at the active site.

2.5 Absorption, Distribution, Metabolism, Elimination and Toxicity (ADMET) Screening

Examination of drug-like properties, pharmacokinetics, and pharmacodynamics parameters of the identified compounds was done using ADMETSAR online software. The canonical smiles of the compounds were obtained from PubChem software and submitted to ADMETSAR [24].

2.6 Molecular Docking

To identify the binding energies of the protein-ligand interaction, molecular docking was performed by binding the 3D structures of the identified compounds on the human androgen receptor (PDB:1e3g). The molecular docking was done using the Autodock Vina found in the PyRx molecular docking software [25]. The docking results (binding energies) were organized in excel spread sheet while the post-docking visualization of the ligand-target interaction was performed in the discovery studio software.

2.7 Density functional theory calculations

UNDER PEER REVIEW

Density functional theory calculations were undertaken using the acceryl density functional theory (DFT) electronic structure DMol3 programs imbibed in the Materials Studio 8.0 software from Acceryl.

3. RESULTS

3.1 Phytochemical Screening Results

FTIR analysis was undertaken on the plant material to identify the functional groups present. The spectrum is presented in Figure 2. The prominent peacks observed in the spectrum include: 3343 cm^{-1} corresponding to N-H bond, 2855.1cm^{-1}, 2922.2 cm^{-1} of C-H bond, 16733.8 cm^{-1}, 1729.5cm^{-1} of C=O and C=C respectively, 1449.9 cm^{-1} C-H bond and 1124 $cm^{-1}$of C-C bond.

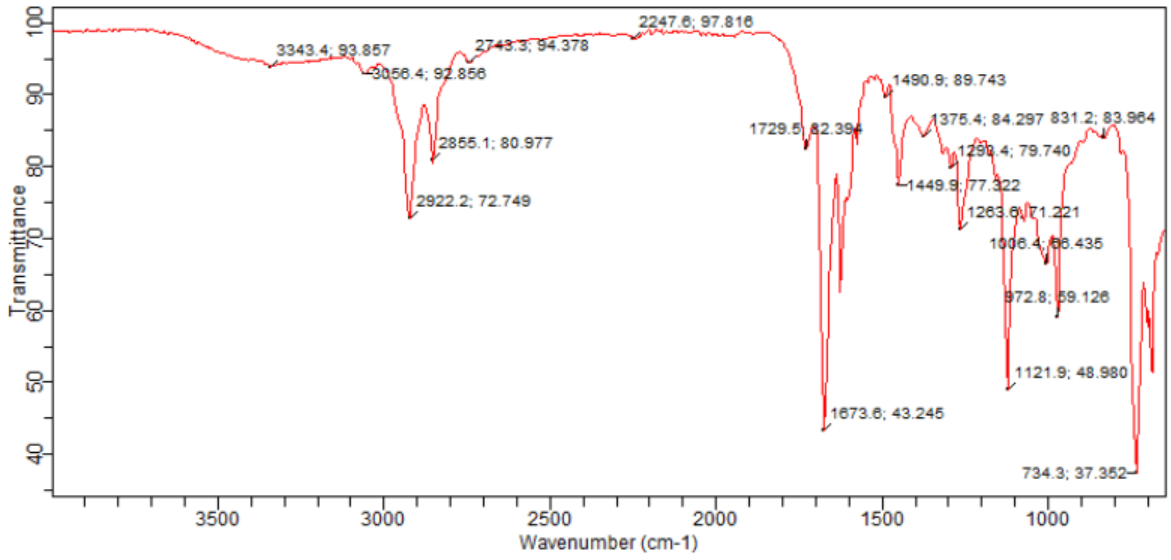

Figure 2. FTIR spectrum of Cinnamomum zeylanicum powder

The GC-MS analysis revealed 31 compounds which are listed in Table 1 while the chromatogram is shown in Figure 3.

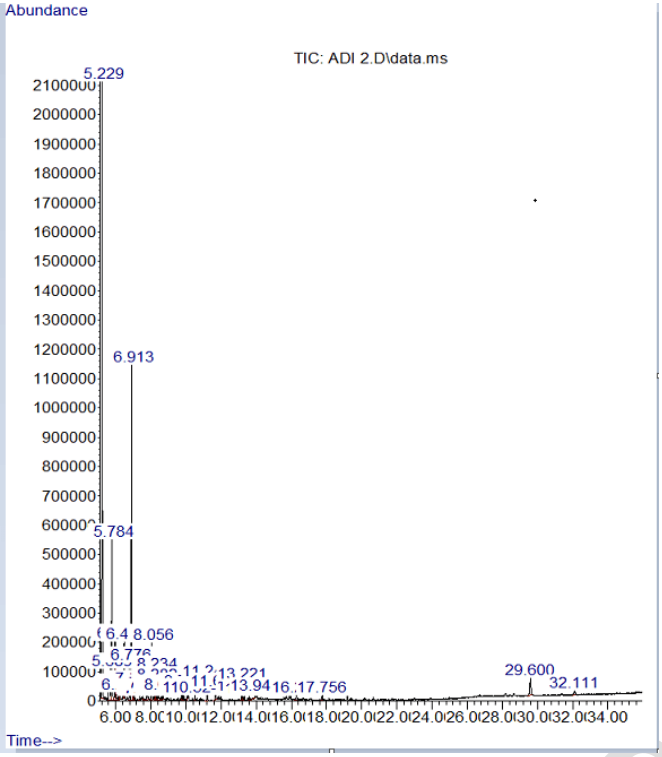

Figure 3 GC-MS chromatogram of *Cinnamomum zeylanicum*

Table 1. Compound identified in the GC-MS analysis and Methyltrienolone as the control drug.

S.no,	Compound	Area peak	Pubchem id	Structure	Molecular formula	Molecular weight
1.	Methyltrienolone	Control	261000	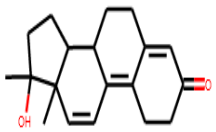	$C_{19}H_{24}O_2$	284
2	Ethanone, 1-[4-(1-methylethyl)phenyl]-	38.3204	12578		$C_{11}H_{14}O$	162.23
3	trans-Cinnamic acid	3.8033	444539	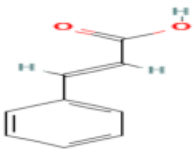	$C_9H_8O_2$	148.16

UNDER PEER REVIEW

4	Coumarin	9.2153	323	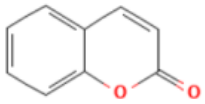	$C_9H_6O_2$	146.14
5	2-Carboxycinnamic acid	3.5487	904938	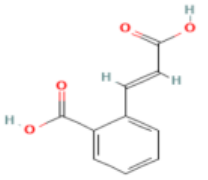	$C_{10}H_8O_4$	192.17
6	Naphthalene, 1,2,4a,5,6,8a-hexahydro-4,7-dimethyl-1-(1-methylethyl)-	0.5261	101708	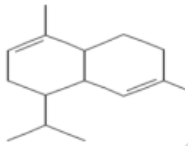	$C_{15}H_{24}$	204.35
7.	Benzene, 1-(1,5-dimethyl-4-hexenyl)-4-methyl-	0.4192	92139	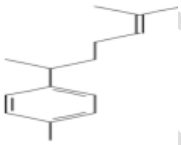	$C_{15}H_{22}$	202.33
8.	.alpha.-Muurolene	5.564	101708	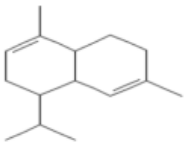	$C_{15}H_{24}$	204.35
9.	2-Propenal, 3-(2-methoxyphenyl)-	20.4485	641298	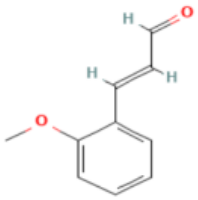	$C_{10}H_{10}O_2$	162.18
10.	.alpha.-Calacorene	0.7418	528708	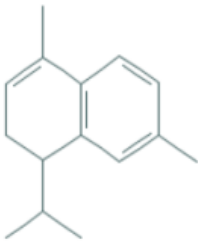	$C_{15}H_{20}$	200.32
11.	Cyclooctane, cyclohexyl-	0.3927	543869		$C_{14}H_{26}$	194.36

UNDER PEER REVIEW

12.	Cyclohexane, 1-ethenyl-1-methyl-2-(1-methylethenyl)-4-(1-methylethylidene)-	0.245	6432312	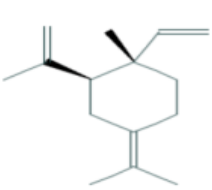	$C_{15}H_{24}$	204.35
13.	3-Cyclohexen-1-carboxaldehyde, 3,4-dimethyl-	0.9413	537551	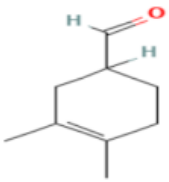	$C_9H_{14}O$	138.21
14.	2H-Indazole, 2-methyl-4-nitro-	3.0644	280212	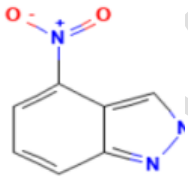	$C_8H_7N_3O_2$	177.16
15.	.tau.-Muurolol	1.5205	3084331	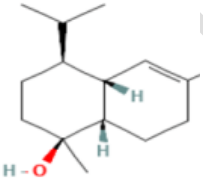	$C_{15}H_{26}O$	222.37
16	Copaene	0.9227	12303902	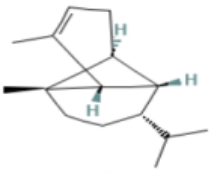	$C_{15}H_{24}$	204.35
17	Tricyclo[5.2.1.0(2,6)]decan-10-ol	0.5396	578081	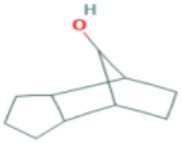	$C_{10}H_{16}O$	152.23
18	Benzaldehyde, 4-hydroxy-3,5-dimethoxy-	0.2592	8655	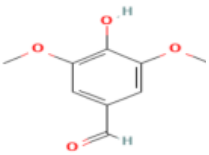	$C_9H_{10}O_4$	182.17
19	Naphthalene, 1,6-dimethyl-4-(1-methylethyl)-	0.4642	10225	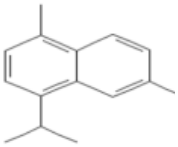	$C_{15}H_{18}$	198.30
20	5,6-Dihydro-2-(4-tolyl)-4H-1,3-oxazin-5-one	0.4643	577139	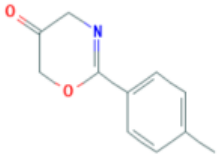	$C_{11}H_{11}NO_2$	189.21

UNDER PEER REVIEW

21	5,6,7,8-Tetramethylbicyclo[4.1.0]hept-4-en-3-one	0.5467	578530	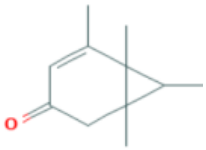	$C_{11}H_{16}O$	164.24
22	13-Octadecenal, (Z)-	0.3517	5364497		$C_{18}H_{34}O$	266.5
23	Tetradecanal	0.1483	31291		$C_{14}H_{28}O$	212.37
24	Cyclopropanecarboxylic acid, (adamantanyl-1)methyl ester	0.2049	585226	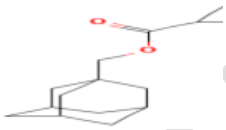	$C_{15}H_{22}O_2$	234.33
25	Hexadecanoic acid, methyl ester	1.1074	8181		$C_{17}H_{34}O_2$	270.5
26	n-Hexadecanoic acid	0.7977	985		$C_{16}H_{32}O_2$	256.42
27	13-Tetradece-11-yn-1-ol	0.3584	543337		$C_{14}H_{24}O$	208.34
28	1,3-Butadiene, 1,4-dimethoxy-, (E,E)-	1.3731	5362907	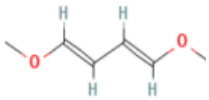	$C_6H_{10}O_2$	114.14
29	2,1,3-Benzoxadiazol-4(5H)-one, 6,7-dihydro-, O-[2-[3,4-dihydro-2(1H)-isoquinolinyl]-2-oxoethyl]oxime	0.3090	9601008		$C_{17}H_{18}N_4O_3$	326.35
30	1,3-Butadiene, 1,4-dimethoxy-, (Z,Z)-	0.4579	5362908	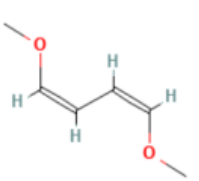	$C_6H_{10}O_2$	114.14

UNDER PEER REVIEW

31	Z,E-3,13-Octadecadien-1-ol	0.3269	5364516	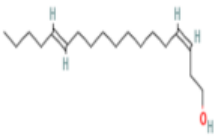	$C_{18}H_{34}O$	266.5
32	Benzenamine, 4-(2-phenylethenyl)-N-(3,5-dimethyl-1-pyrazolylmethyl)-	2.6169	680405	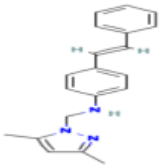	$C_{20}H_{21}N_3$	303.4

3.2 ADMET Result

Absorption, distribution, metabolism, elimination and toxicity examination was performed on the compounds. The ADMET properties showing their pharmacodynamics and pharmacokinetics are summarized in Table 2. Interestingly, none of the compounds violated more than one of the Lipinski s rule [26]. According to the rule an orally administered drug should not have more than 5 hydrogen bond donors, more than 10 hydrogen bond acceptors and should have a molecular mass less than 500, Majority of the compounds show positive human intestine absorption indicating that they can be better taken from the gastrointestinal tract when consumed orally. Only two of the compounds were found to show carcinogenic properties. The blood brain barrier (BBB) penetration study was performed, the result indicated that four of the compounds gave negative result to penetrate blood brain; the obtained results indicated that the plant material could be a drug lead candidate.

Table 2. Absorption, distribution, metabolism, elimination and toxicity Table

s/no	**Compound**	**HIA**	**BBB**	**H-bond acceptor**	**H-bond donor**	**Rotatable bonds**	**Carcinogenicity**
1	Methyltrienolone	+	-	2	1	0	-
2	Ethanone, 1-[4-(1-methylethyl)phenyl]-	+	+	1	0	2	-
3	trans-Cinnamic acid	+	+	1	1	2	+
4	Coumarin	+	-	2	0	0	-
5	2-Carboxycinnamic acid	+	+	2	2	3	-

UNDER PEER REVIEW

6	Naphthalene, 1,2,4a,5,6,8a-hexahydro-4,7-dimethyl-1-(1-methylethyl)-	+	+	0	0	1	-
7	Benzene, 1-(1,5-dimethyl-4-hexenyl)-4-methyl-	+	+	0	0	4	-
8	.alpha.-Muurolene	+	+	0	0	1	-
9	2-Propenal, 3-(2-methoxyphenyl)-	+	-	2	0	3	-
10	.alpha.-Calacorene	+	+	0	0	1	-
11	Cyclooctane, cyclohexyl-	+	+	0	0	1	-
12	Cyclohexane, 1-ethenyl-1-methyl-2-(1-methylethenyl)-4-(1-methylethylidene)-	+	+	0	0	2	-
13	3-Cyclohexen-1-carboxaldehyde, 3,4-dimethyl-	+	+	1	0	1	-
14	2H-Indazole, 2-methyl-4-nitro-	+	+	4	0	1	-
15	.tau.-Muurolol	+	+	1	1	1	-
16	Copaene	+	+	0	0	1	-
17	Tricyclo[5.2.1.0 (2,6)]decan-10-ol	+	+	1	1	0	-
18	Benzaldehyde, 4-hydroxy-3,5-dimethoxy-	+	-	4	1	3	-
19	Naphthalene, 1,6-dimethyl-4-(1-methylethyl)-	+	+	0	0	1	-
20	5,6-Dihydro-2-(4-tolyl)-4H-1,3-oxazin-5-one	+	+	3	0	1	-
21	5,6,7,8-Tetramethylbicyclo[4.1.0]hept-4-en-3-one	+	+	1	0	0	-
22	13-Octadecenal, (Z)-	+	+	1	0	15	-
23	Tetradecanal	+	+	1	0	12	-

UNDER PEER REVIEW

24	Cyclopropanecarboxylic acid, (adamantanyl-1)methyl ester	+	+	2	0	3	-
25	Hexadecanoic acid, methyl ester	+	+	2	0	14	-
26	n-Hexadecanoic acid	+	+	1	1	14	-
27	13-Tetradece-11-yn-1-ol	+	+	1	1	9	-
28	1,3-Butadiene, 1,4-dimethoxy-, (E,E)-	+	+	2	0	3	+
28	2,1,3-Benzoxadiazol-4(5H)-one, 6,7-dihydro-, O-[2-[3,4-dihydro-2(1H)-isoquinolinyl]-2-oxoethyl]oxime	+	+	6	0	3	-
30	1,3-Butadiene, 1,4-dimethoxy-, (Z,Z)-	+	+	2	0	3	-
31	Z,E-3,13-Octadecadien-1-ol	+	+	1	1	14	-
32	Benzenamine, 4-(2-phenylethenyl)-N-(3,5-dimethyl-1-pyrazolylmethyl)-	+	+	3	1	5	-

HIA=Human intestinal absorption, BBB= Blood Brain Barrier

3.3 Molecular docking data

Computational molecular docking study was performed to identify the target-ligand interaction effects between the chosen human androgen receptor (PDB:1e3g) and the identified compounds. The docking binding energies are tabulated in Table 3 as well as the 3-dimentional (3D) and 2-dimentional (2D) protein-ligand interactions. Copaene gave the lowest binding score ($-8.2\ Kcal\ mol^{-1}$), better than Methyltrienolone which was used as the control and gave binding energy of -6.8 $Kcal\ mol^{-1}$. The amino acids involved in the ligand-target interactions as well as the force of interactions involved are presented in Table 4. Major forces of interactions observed include Conventional hydrogen bond, unfavorable ecceptor-ecceptor, alkyl, pi-alkyl, Pi-cation, pi-pi stacked and pi-sigma.

UNDER PEER REVIEW

Table 3 Target-Ligand interactions of identified compounds

S/No.	Pubchem id	Name of compound	Docking score (kCal/mol)	3D and 2D protein ligand interactions	
				3D	2D
1	261000	Methyltrienolone	-6.8	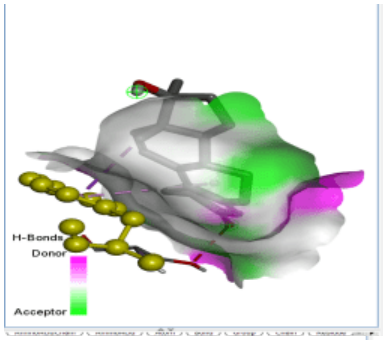	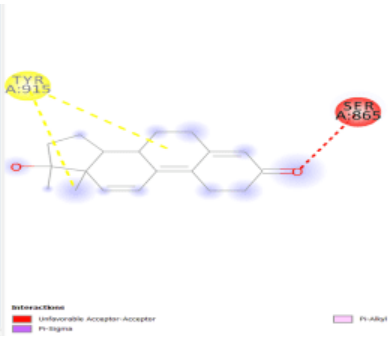
2	12578	Ethanone, 1-[4-(1-methylethyl)phenyl]-	-6.6	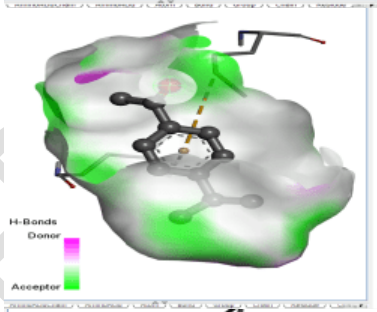	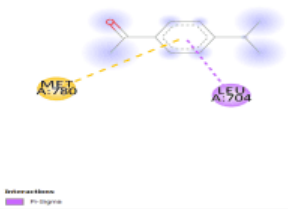
3	444539	trans-Cinnamic acid	-6.6	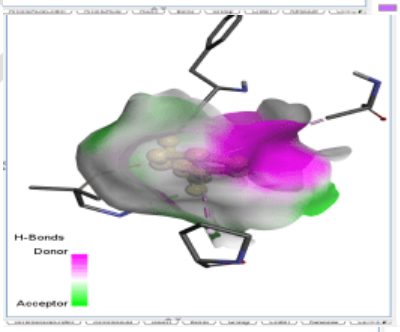	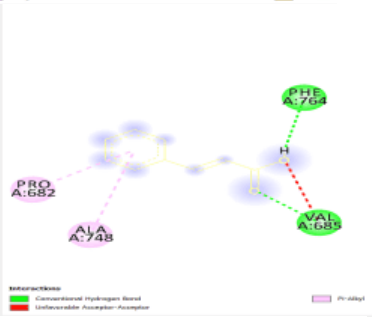
4	323	Coumarin	-7.0	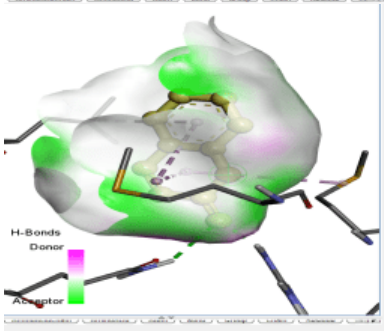	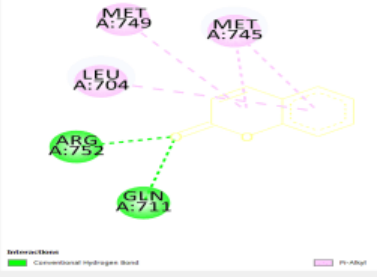

UNDER PEER

5	904938	2-Carboxycinnamic acid	-7.1	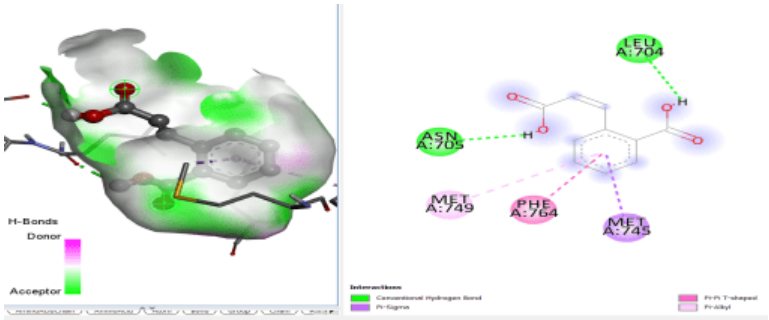
6	101708	Naphthalene, 1,2,4a,5,6,8a-hexahydro-4,7-dimethyl-1-(1-methylethyl)-	-7.6	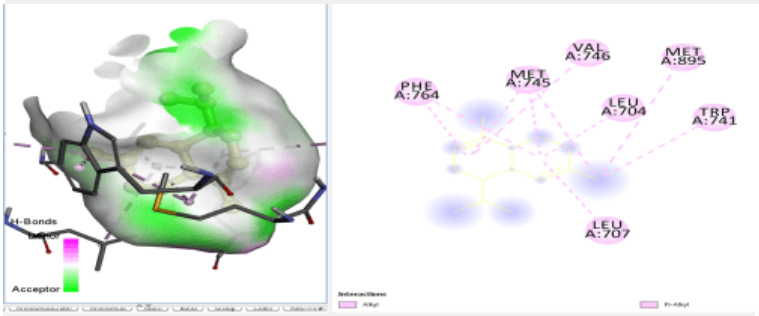
7	92139	Benzene, 1-(1,5-dimethyl-4-hexenyl)-4-methyl-	-6.6	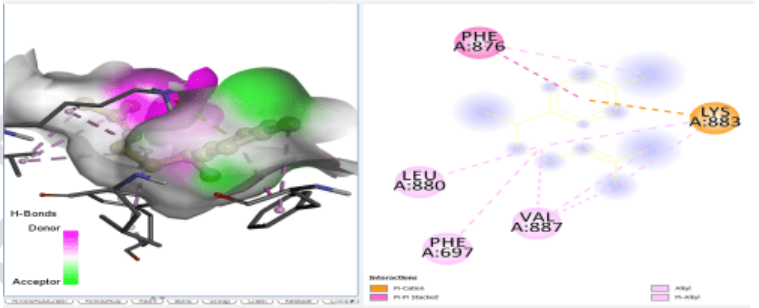
8.	101708	.alpha.-Muurolene	-7.1	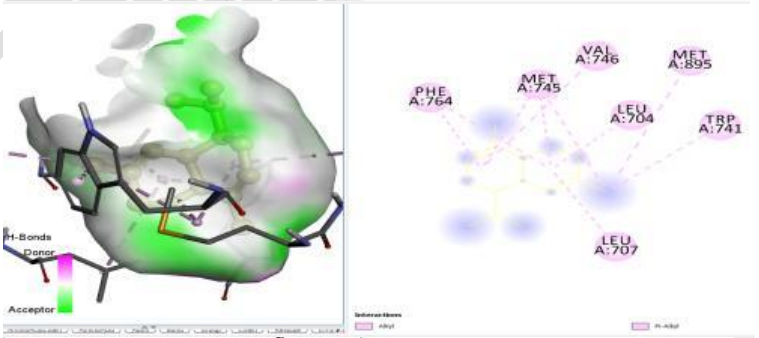
9	641298	2-Propenal, 3-(2-methoxyphenyl)-	-6.0	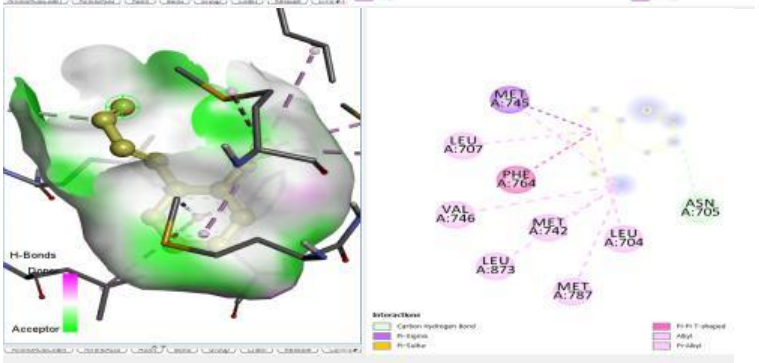

UNDER PEER

10	528708	.alpha.-Calacorene	-7.6	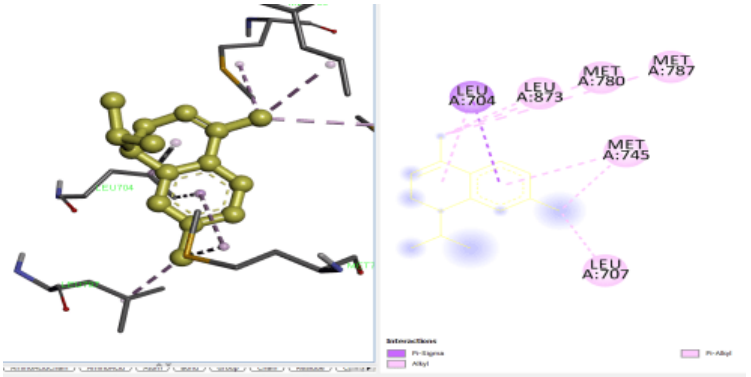
11	543869	Cyclooctane, cyclohexyl-	-8.0	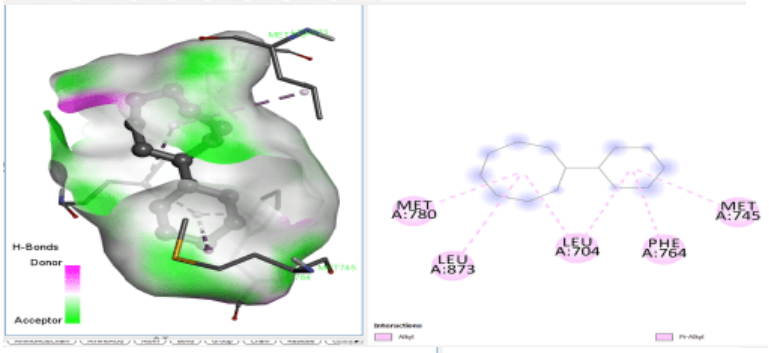
12	6432312	Cyclohexane, 1-ethenyl-1-methyl-2-(1-methylethenyl)-4-(1-methylethylidene)-	-7.6	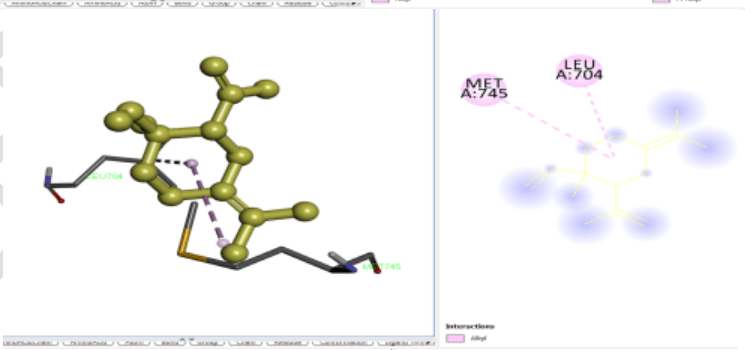
13	537551	3-Cyclohexen-1-carboxaldehyde, 3,4-dimethyl-	-5.8	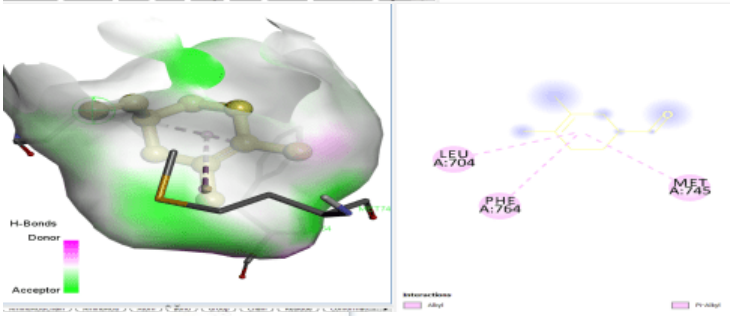
14	280212	2H-Indazole, 2-methyl-4-nitro-	-7.2	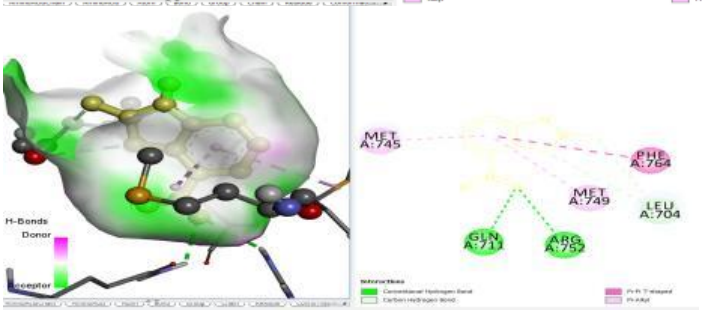

UNDER PEER

15	3084331	.tau.-Muurolol	-7.0	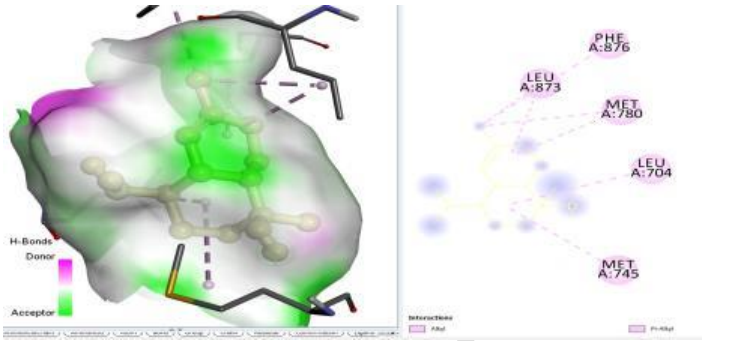
16	12303902	Copaene	-8.2	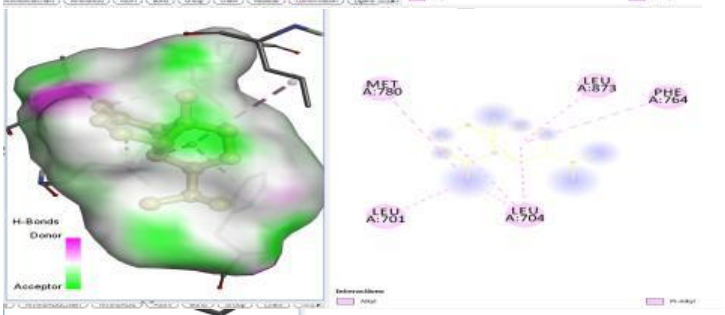
17	578081	Tricyclo[5.2.1.0(2,6)]decan-10-ol	-6.3	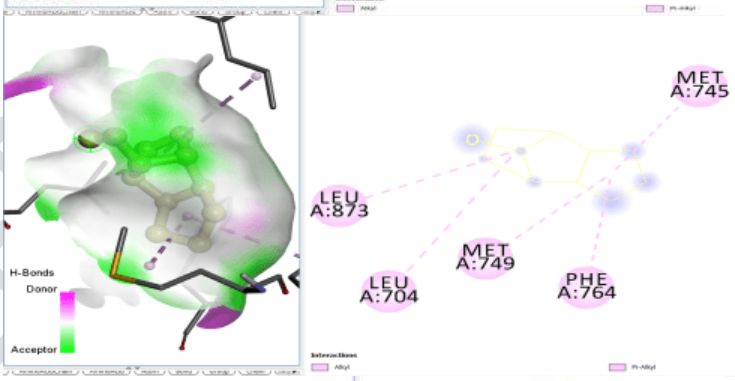
18	8655	Benzaldehyde, 4-hydroxy-3,5-dimethoxy-	-5.7	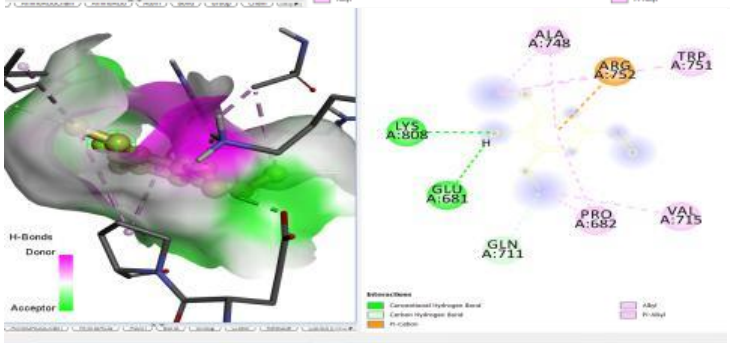
19	10225	Naphthalene, 1,6-dimethyl-4-(1-methylethyl)-	-7.1	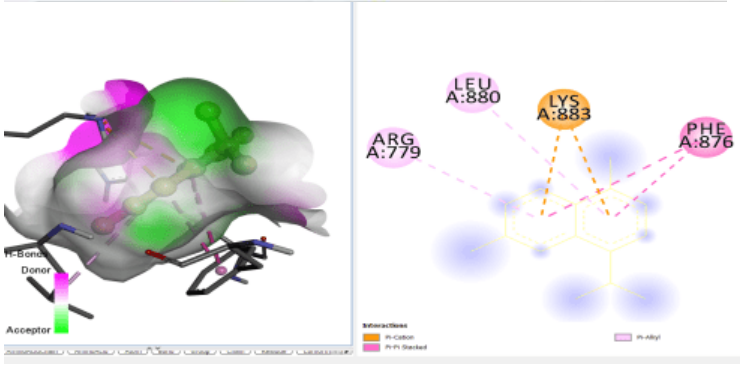

UNDER PEER

20	577139	5,6-Dihydro-2-(4-tolyl)-4H-1,3-oxazin-5-one	-7.8	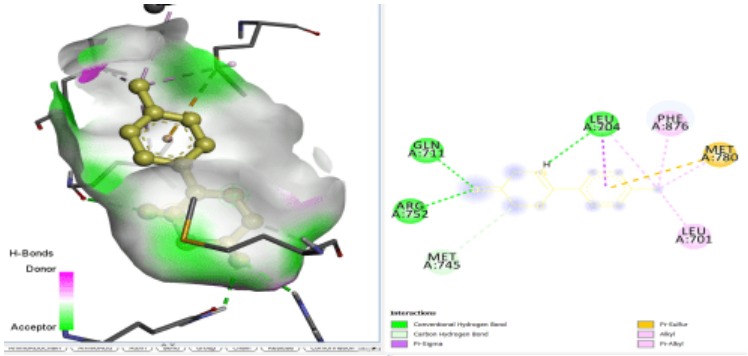
21	578530	5,6,7,8-Tetramethylbicyclo[4.1.0]hept-4-en-3-one	-5.0	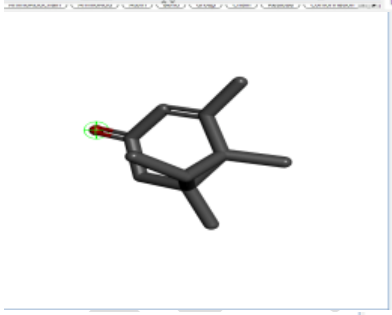 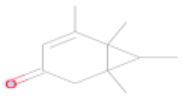
22	5364497	13-Octadecenal, (Z)-	-5.0	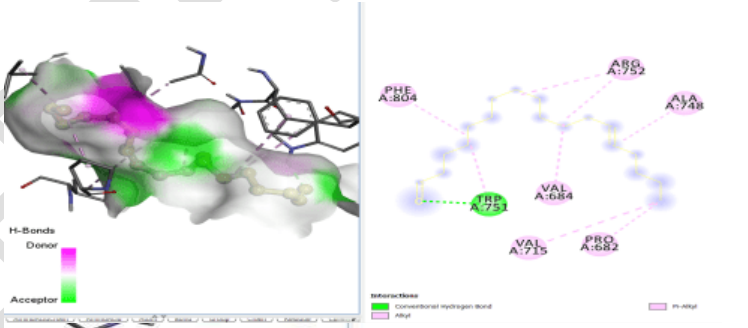
23	31291	Tetradecanal	-4.7	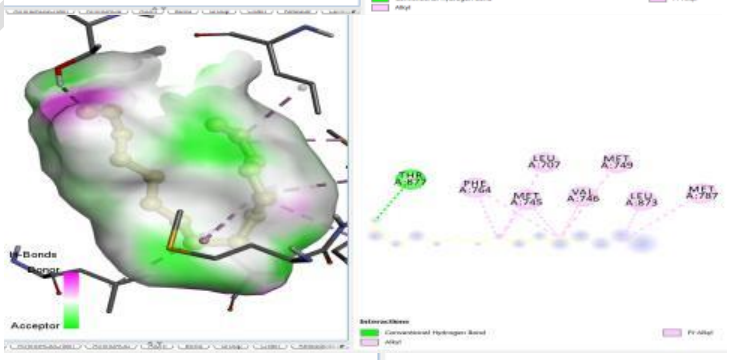
24	585226	Cyclopropanecarboxylic acid, (adamantanyl-1)methyl ester	-7.2	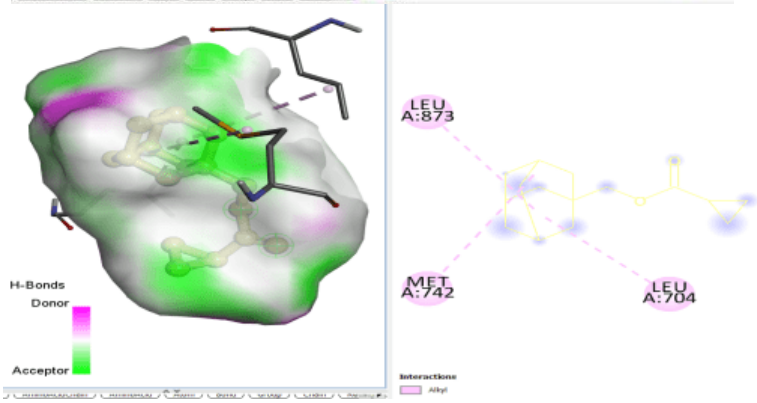

UNDER PEER

25	8181	Hexadecanoic acid, methyl ester	-5.2	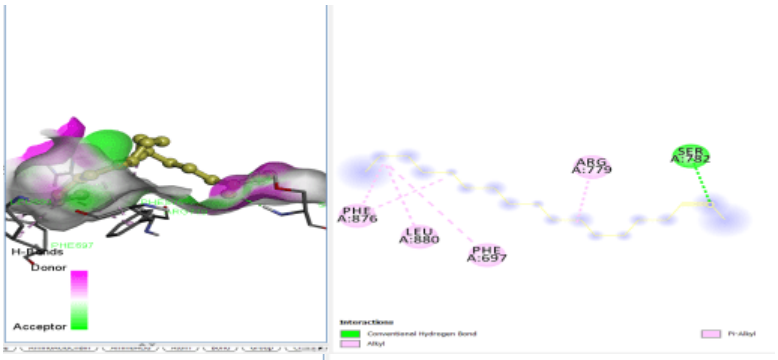
26	985	n-Hexadecanoic acid	-4.7	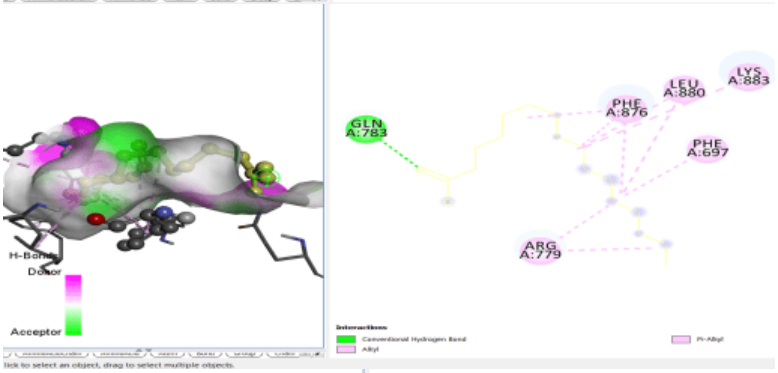
27	543337	13-Tetradece-11-yn-1-ol	-4.2	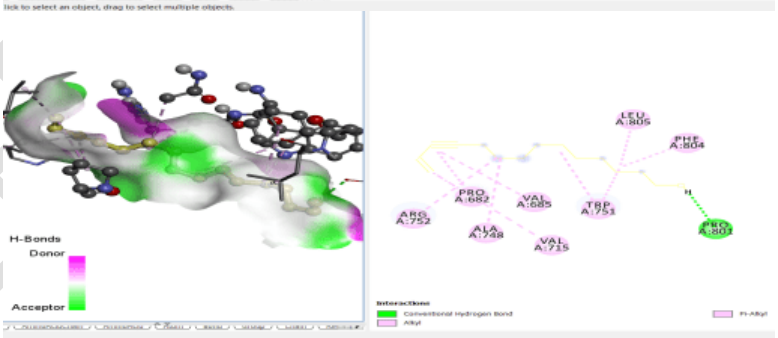
28	5362907	1,3-Butadiene, 1,4-dimethoxy-, (E,E)-	-3.9	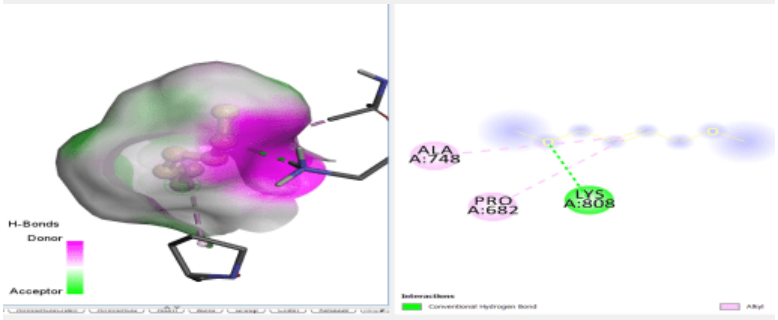
29	9601008	2,1,3-Benzoxadiazol-4(5H)-one, 6,7-dihydro-, O-[2-[3,4-dihydro-2(1H)-isoquinolinyl]-2-oxoethyl]oxime	-7.1	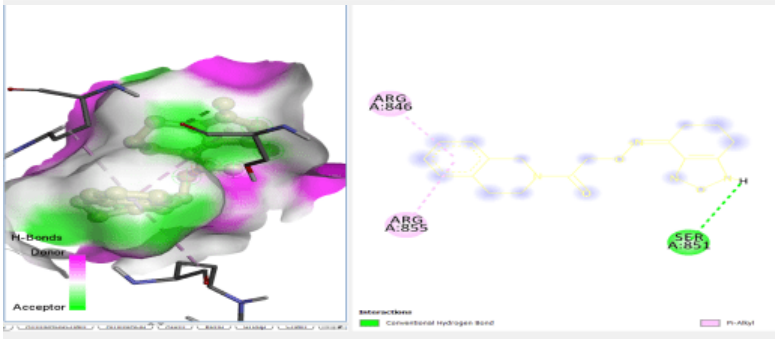

UNDER PEER

30	5362908	1,3-Butadiene, 1,4-dimethoxy-, (Z,Z)-	-4.1
31	5364516	Z,E-3,13-Octadecadien-1-ol	-5.5
32	680405	Benzenamine, 4-(2-phenylethenyl)-N-(3,5-dimethyl-1-pyrazolylmethyl)-	-7.9

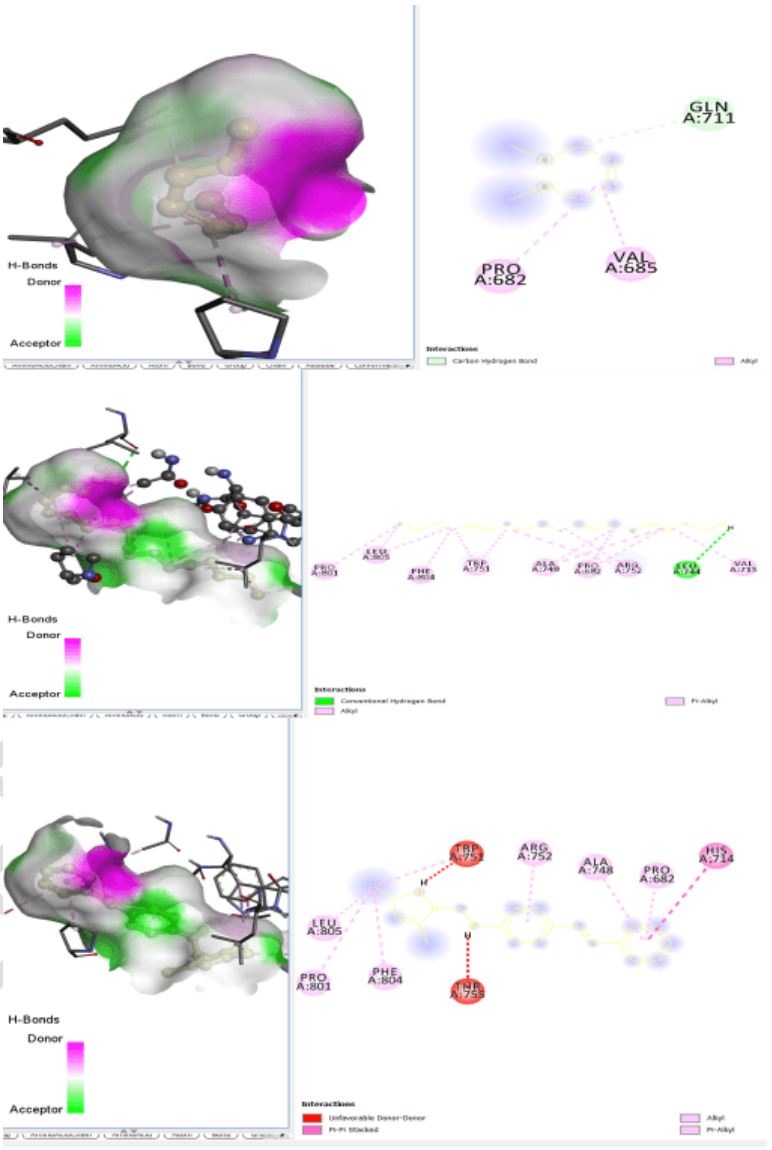

Table 4. Amino acid residues and forces of interactions between the target and ligands

S/no.	Compound	Amino acid involved	Type of interaction
1.	Methyltrienolone	TYR 915, SER 865	Unfavorable acceptor-acceptor, pi-alkyl, pi-sigma
2.	Ethanone, 1-[4-(1-methylethyl)phenyl]-	MET 780, LEU 704	Pi-sigma, pi-suffur
3.	trans-Cinnamic acid	ALA748, PHE 764, PRO 682, VAL 685	Conventional hydrogen bond, unfavorable ecceptor-ecceptor, pi-alkyl
4.	Coumarin	ARG 752, GLN 711,	conventional hydrogen

UNDER PEER

		LEU 704, MET 749, MET 745,	bond, pi-alkyl
5.	2-Carboxycinnamic acid	ASN 705,LEU 704,MET 745, MET 749, PHE 764	conventional hydrogen bond, pi-alkyl, Pi-sigma, pi-pi –shaped
6	Naphthalene, 1,2,4a,5,6,8a-hexahydro-4,7-dimethyl-1-(1-methylethyl)-	LEU 704, LEU 707, MET 745, MET 895, PHE 764, TRP 741, VAL 746	Alkyl, pi-alkyl
7	Benzene, 1-(1,5-dimethyl-4-hexenyl)-4-methyl-	LEU 880, PHE 697, PHE 876, LYS 883, VAL 887	Pi-cation, alkyl, pi-alkyl, pi-pi stacked
8	.alpha.-Muurolene	LEU 704, LEU 707, MET 745, MET 895, PHE 764, TRP 741, VAL 746	Alkyl, pi-alkyl
9	2-Propenal, 3-(2-methoxyphenyl)-	ASN 705, LEU 704, LEU707, MET 742, MET 745, MET 787PHE 764, VAL 746	carbon-hydrogen bond, alkyl, pi-alkyl, pi-suffur, pi-sigma, pi-pi T-shaped
10	.alpha.-Calacorene	LEU 704, LEU 707, LEU 873, MET 745, MET 780, MET 787	Alkyl, pi-alkyl, pi-sigma
11	Cyclooctane, cyclohexyl-	LEU 704, LEU 873, MET 745, MET 780, PHE 764	Alkyl, pi-alkyl
12	Cyclohexane, 1-ethenyl-1-methyl-2-(1-methylethenyl)-4-(1-methylethylidene)-	LEU 704, MET 745	Alkyl
13	3-Cyclohexen-1-carboxaldehyde, 3,4-dimethyl-	LEU 704, MET 745,	alkyl, pi-alkyl
14	2H-Indazole, 2-methyl-4-nitro-	ARG 752, GLN 711 LEU 704, MET 745, MET 749, PHE 764,	conventional hydrogen, carbon hydrogen, pi-alkyl, pi-pi Tshaped
15	.tau.-Muurolol	LEU 704, LEU 873, MET 745, MET780,PHE 876	alkyl, pi-alkyl

UNDER PEER REVIEW

16	Copaene	LEU 701, LEU 704, LEU 873, MET 780, PHE 764	Alkyl, pi-alkyl
17	Tricyclo[5.2.1.0 (2,6)]decan-10-ol	LEU 704, LEU 873, MET 745, MET 749, PHE 764	Alkyl, pi-alkyl
18	Benzaldehyde, 4-hydroxy-3,5-dimethoxy-	ALA 748,ARG 752, GLU 681, GLN 711, LYS 808, PRO 682, TRP 751, VAL 715	Conventional hydrogen bond, carbon hydrogen Alkyl, pi-alkyl, pi-cation
19	Naphthalene, 1,6-dimethyl-4-(1-methylethyl)-	ARG 778, LEU 880,LYS 883, PHE 879	Alkyl,pi-alkyl, pi-pi stacked
20	5,6-Dihydro-2-(4-tolyl)-4H-1,3-oxazin-5-one	AGR 752, GLN 711, LEU 701, LEU 704, MET 745, MET 780, PHE 876,	conventional hydrogen, carbon hydrogen, pi-alkyl, pi-suffur,pi-sigma, pi-alkyl
21	5,6,7,8-Tetramethylbicyclo[4.1.0]hept-4-en-3-one	Nil	Nil
22	13-Octadecenal, (Z)-	ALA 748, ARG 752, PHE 804, PRO 682, TRP 751, VAL 715, VAL 684,	Conventional hydrogen bond, alkyl, pi-alkyl
23	Tetradecanal	LEU 707, LEU 873,MET 745, MET 749, MET 787, PHE 764, THR 877, VAL 746	Conventional hydrogen bond, alkyl, pi-alkyl
24	Cyclopropanecarboxylic acid, (adamantanyl-1)methyl ester	LEU 704, LEU 873, MET 742	Alkyl
25	Hexadecanoic acid, methyl ester	ARG 779, LEU 880, PHE 697, PHE 876, SER 782	Conventional hydrogen bond, alkyl pi-alkyl
26	n-Hexadecanoic acid	ARG 779, GLN 783, LEU 880, PHE 697, PHE 876, LYS 883	Conventional hydrogen bond, alkyl pi-alkyl
27	13-Tetradece-11-yn-1-ol	ALA 748, ARG 752 LEU 805, PHE 804, PRO 682, PRO 801,	Conventional hydrogen bond, alkyl, pi-alkyl

UNDER PEER REVIEW

		TRP 751, VAL 685, VAL 715	
28	1,3-Butadiene, 1,4-dimethoxy-, (E,E)-	ALA 748, LYS 808, PRO 682	Conventional hydrogen bond, alkyl
29	2,1,3-Benzoxadiazol-4(5H)-one, 6,7-dihydro-, O-[2-[3,4-dihydro-2(1H)-isoquinolinyl]-2-oxoethyl]oxime	AGR 846, AGR 855, SER 851	Conventional hydrogen bond, alkyl
30	1,3-Butadiene, 1,4-dimethoxy-, (Z,Z)-	GLN 711, PRO 682, VAL 685	Carbon hydrogen bond, alkyl
31	Z,E-3,13-Octadecadien-1-ol	ALA 748,ARG 752, LEU 744, LEU 805, PHE 804, PRO 682, PRO 801,TRP 751,VAL 715	Conventional hydrogen bond, alkyl, pi-alkyl
32	Benzenamine, 4-(2-phenylethenyl)-N-(3,5-dimethyl-1-pyrazolylmethyl)-	ALA 748, ARG 752, LEU 805, HIS 714, PHE 804, PRO 682, PRO 801, TRP 752, THR 755	Unfavorable donor-donor, alkyl, pi-alkyl, pi-pi stacked

3.4 Density functional theory results

To ascertain the relationship between the structures of the compounds and their reactivity, density functional theory calculations were undertaken. The calculations were performed in the electronic structure DMol^3 program in the frame work of the Perdew-Wang (PW) local correlation density functional, Mulliken population analysis, and the DND basis set [27], geometric optimization was performed on the structures prior to frontier orbital calculations. The compounds with area peaks greater than 1 % were selected for the DFT studies. Figure 4 shows the optimized structures and the frontier orbitals while Table 5 revealed the electronic properties of the compounds. The highest occupied molecular orbital (HOMO) and the lowest unoccupied molecular orbitals (LUMO) also known as the frontier molecular orbitals are employed in predicting the most reactive regions in a molecule, they are used in describing the chemical reactivity patterns of molecules [28], the HOMO orbital is rich in electron and has a tendency to donate to electron unoccupied region whereas the HOMO orbital is electron deficient region ready to accept from the electron rich environment, the gap energy (HOMO-LUMO) is related to the kinetic stability and chemical reactivity of the molecules studied [29] hence a molecule with small gap energy will show high polarizability and good chemical reactivity as well as low kinetic stability, and is qualified to be classified as a soft molecule. Using the HOMO and

UNDER PEER REVIEW

LUMO energies the quantum chemical descriptor including hardness (η), softness (δ) and electronegativity (χ) were calculated using the equations below:

$$\chi = \frac{IP+EA}{2} \quad (1)$$

$$\eta = \frac{IP-EA}{2} \quad (2)$$

$$\delta = \frac{1}{\eta} \quad (3)$$

Where IP represents the ionization potential and EA is the electron affinity, the hardness shows the tendency of the compound to resist the transfer of electron, it is an indication of good chemical reactivity, the softness shows the tendency of a chemical compound to draw electron to its and the electronegativity shows the compounds ability to attract electron to itself when participating in a covalent bond system. The calculated values of the quantum chemical descriptors shown in Table show that the compounds would have good reactivity towards the drug target.

UNDER PEER REVIEW

Compound	Optimized structure	HOMO orbital	LUMO orbital
Methyltrienolone	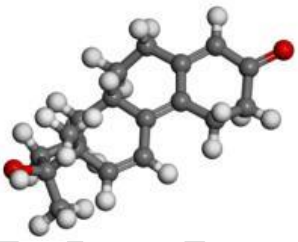	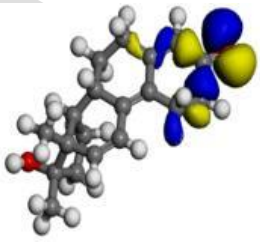	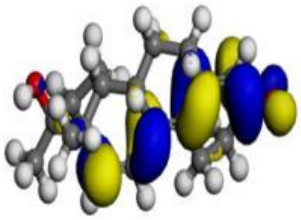
Ethanone, 1-[4-(1-methylethyl)phenyl]-	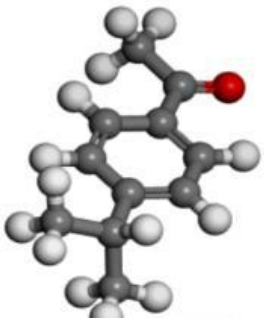	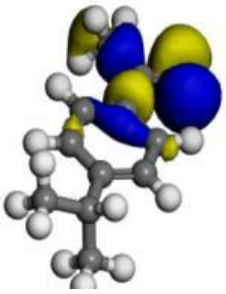	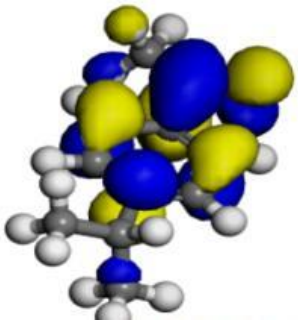
trans-Cinnamic acid	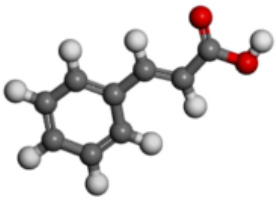	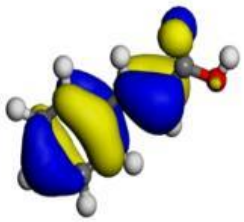	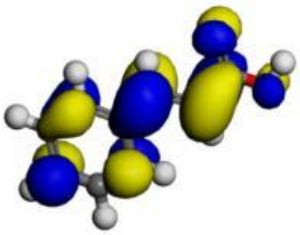

Coumarin

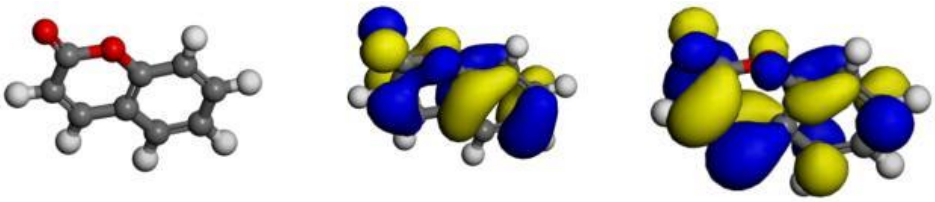

2-Carboxycinnamic acid

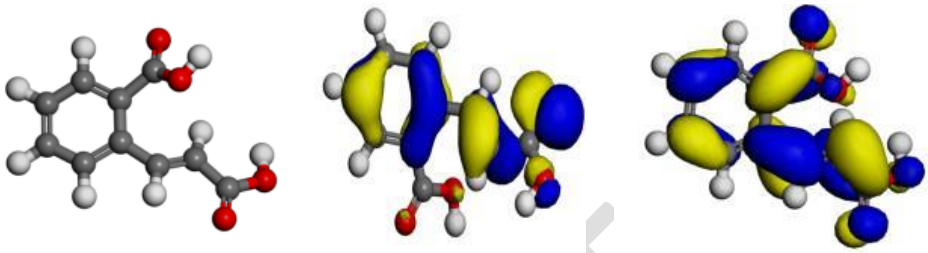

alpha.-Muurolene

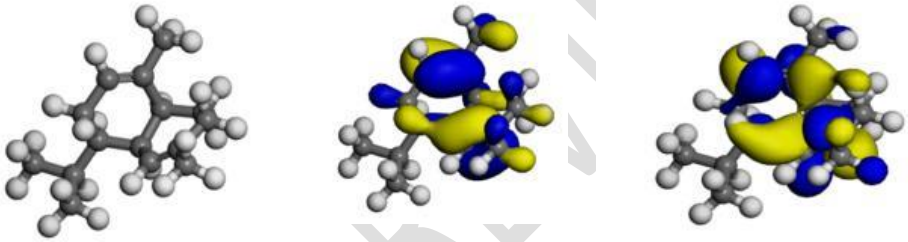

2-Propenal, 3-(2-methoxyphenyl)-

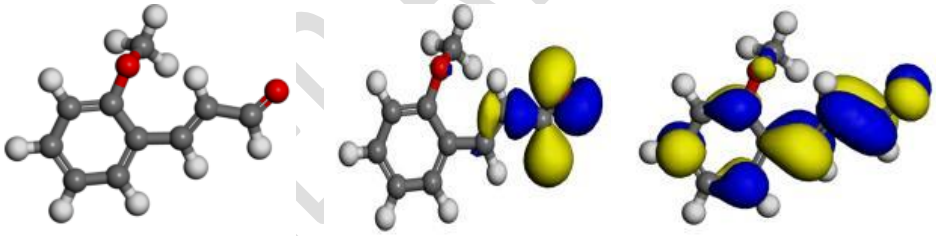

Hexadecanoic acid, methyl ester

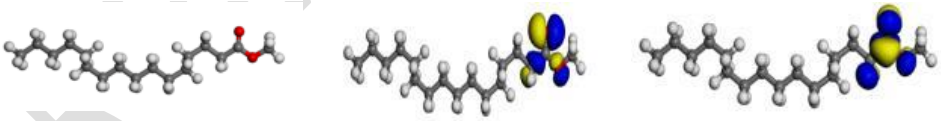

1,3-Butadiene, 1,4-dimethoxy-, (E,E)-

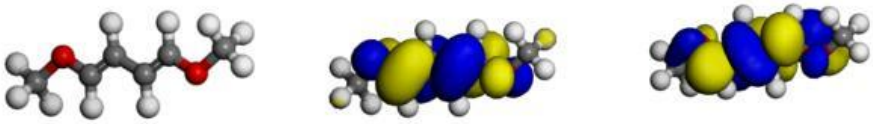

2,1,3-Benzoxadiazol-4(5H)-one, 6,7-dihydro-, O-[2-[3,4-dihydro-2(1H)-isoquinolinyl]-2-oxoethyl]oxime

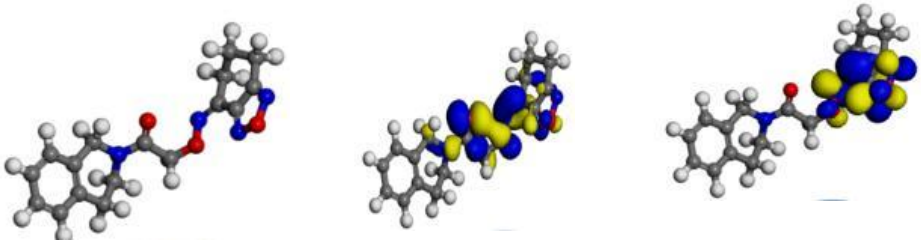

Benzenamine, 4-(2-phenylethenyl)-N-(3,5-dimethyl-1-pyrazolylmethyl)-

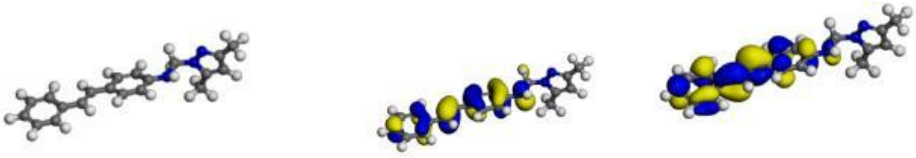

Figure 4. density functional theory properties of some of the selected compounds, optimized structures, HOMO and LUMO orbitals.(atom legend: white-H, light gray-C and pink-O)

Table 5. quantum chemical descriptor of the selected compounds

Compound	E_{HOMO} (eV)	E_{OMO} (eV)	**IP= - E_{HOMO}**	**EA= - E_{LUMO}**	**Energy gap** $(E_{LUMO} - E_{HOMO})$ (eV)	χ	η	δ
Methyltrienolone	-5.0340	-2.8027	5.0340	2.8027	2.2313	3.9184	1.1157	0.8963
Ethanone, 1-[4-(1-methylethyl)phenyl]-	-5.5238	-2.3946	5.5238	2.3946	3.1292	3.9592	1.5646	0.6391
trans-Cinnamic acid	-6.0401	-2.8300	6.0401	2.8300	3.2101	4.4351	1.6051	0.6230
Coumarin	-6.0681	-2.8572	6.0681	2.8572	3.2109	4.4627	1.6055	0.6229
2-Carboxycinnamic acid	-6.3674	-3.2653	6.3674	3.2653	3.1021	4.8164	1.5511	0.6447
.alpha.-Muurolene	-5.1701	-0.2177	5.1701	0.2177	4.9524	2.6939	2.4762	0.4038
2-Propenal, 3-(2-methoxyphenyl)-	-5.5238	-3.0748	5.5238	3.0748	2.4490	4.2993	1.2245	0.8167
Hexadecanoic acid, methyl ester	-6.2857	-0.8245	6.2857	0.8245	5.4612	3.5551	2.7306	0.36621
1,3-Butadiene, 1,4-dimethoxy-, (E,E)-	-4.1360	-0.7612	4.1360	0.7612	3.3748	2.4486	1.6874	0.5926

UNDER PEER REVIEW

2,1,3-Benzoxadiazol-4(5H)-one, 6,7-dihydro-, O-[2-[3,4-dihydro-2(1H)-isoquinolinyl]-2-oxoethyl]oxime	-5.5782	-2.4762	5.5782	2.4762	3.102	4.0272	1.5510	0.6447
Benzenamine, 4-(2-phenylethenyl)-N-(3,5-dimethyl-1-pyrazolylmethyl)-	-4.5170	-1.9591	4.5170	1.9591	2.5579	3.2381	1.2790	0.7819

Conclusion

The extract constituents of *Cinnamomum zeylanicum* were extracted in chloroform; FTIR examination performed on the sample showed that it contained some functional groups which are favorable to drug formulation. The GC-MS result revealed that the plant contained 32 compounds with favorable pharmacological and pharmacodynamics properties to humans. The molecular docking result using Methyltrienolone as control drug showed that copaene gave the lowest binding score (-8.2 k cal mol^{-1}) which is an indication that the plant could be a good drug candidate for prostate cancer control. Density functional theory calculations were performed on some of the compounds identified in the GC-MS analysis, the low values of the energy gap confirmed the chemical reactivities of the molecules towards the drug target. Generally, the values of the calculated quantum chemical descriptors indicated that the plant would be a good drug lead candidate.

UNDER PEER REVIEW

References

1. Jimmy C L, Stephanie C E, Prostate Gland, Encyclopedia of Reproduction (Second Edition), 201 Textbook of Veterinary Diagnostic Radiology (Seventh Edition), 2018
2. Jemal A, Center M M, DeSantis C, Ward E M. Global patterns of cancer incidence and mortality rates and trends. Cancer Epidemiology, Biomarkers & Prevention. 2010, 19(8): 1893-907.
3. Mattiuzzi C, Lippi G. Current Cancer Epidemiology. Journal of epidemiology Global Health.; 2019, 9(4): 217-222.
4. Bray F, Ferlay J, Soerjomataram I, Siegel R, Torre L, Jemal A. Global cancer statistics 2018: GLOBOCAN estimates of incidence and mortality worldwide for 36 cancers in 185 countries. CA Cancer Journal of Clinicians. 2018, 68 (6): 394 – 424. https://doi.org/https://doi.org/10.3322/caac.21492
5. Li Y, Ahmad A, Kong D, et al. Recent progress on nutraceutical research in prostate cancer. Cancer Metastasis Revelation. 2014, 33(2–3): 629–640. doi: 10.1007/s10555-013-9478-9.
6. Pendleton J M, Tan W W, Anai S, et al., Phase II trial of isoflavone in prostate-specific antigen recurrent prostate cancer after previous local therapy. BMC Cancer. 2008; 8 doi: 10.1186/1471-2407-8-132. 132–2407-8–132
7. Tavsan Z, Kayali HA. Flavonoids showed anticancer effects on the ovarian cancer cells: involvement of reactive oxygen species, apoptosis, cell cycle and invasion. Biomedical Pharmacother. 2019, 116: 109004
8. Faezeh T 1 , Shahin A, Shahram L, Parvin K, Ali A, In-silico activity prediction and docking studies of some flavonoid derivatives as anti-prostate cancer agents based on Monte Carlo optimization. BMC Chemistry. 2023, 17:87.
9. Ranasinghe P, Pigera S, Premakumara GA, Galappaththy P, Constantine G R, Katulanda P. Medicinal properties of 'true' cinnamon (Cinnamomum zeylanicum): a systematic review. BMC Complementary and alternative Medicine. 2013, 2213, 275. doi: 10.1186/1472-6882-13-275. PMID: 24148965; PMCID: PMC3854496.
10. Pallavi K, Rathai R, Cinnamon: Mystic powers of a minute ingredient, Pharmacognosy Research. 2015, 7,
11. Reichard P, Nilsson B Y, Rosenqvist U. The effect of long-term intensified insulin treatment on the development of microvascular complications of diabetes mellitus. N England Journal of Medicine. 329 (1993) 304-9.
12. Skyler J S. Effects of glycemic control on diabetes complications and on the prevention of diabetes. Clinical Diabetes. 2004, 22 :162-6.
13. Han D C, Lee M Y, Shin K D, Jeon S B, Kim J M, Son K H, et al. 2'-benzoyloxycinnamaldehyde induces apoptosis in human carcinoma via reactive oxygen species. Journal of biological Chemistry. 2004, 279 (69): 11-20.
14. Kwon H K, Jeon W K, Hwang J S, Lee C G, So J S, Park J A, et al. Cinnamon extract suppresses tumor progression by modulating angiogenesis and the effector function of CD8+ T cells. Cancer Letters 2009, 278: 174-82.

UNDER PEER REVIEW

15. Meng X Y, Zhang H X, Mezei M, Cui M, Molecular docking: a powerful approach for structure-based drug discovery. Current Computational Aided Drug Des. 2011, 7(2): 46-57. doi: 10.2174/157340911795677602. PMID: 21534921; PMCID: PMC3151162.
16. Agu P C, Afiukwa C A, Orji OU. et al. Molecular docking as a tool for the discovery of molecular targets of nutraceuticals in diseases management. Scientific reports. 2023, 13: 13398. https://doi.org/10.1038/s41598-023-40160-2
17. Sahoo R N, Pattanaik S, Pattnaik G, Mallick S, Mohapatra R, Review on the use of molecular docking as the first line tool in drug discovery and development. Indian Journal of Pharmaceutical Sciences. 2022, 84 (5) :1334–1337
18. Jain A N, Virtual screening in lead discovery and optimization. Current Opinion in Drug Discovery and Development. 2004, 7(4):396–403.
19. Ikpa C B C, Ikezu U J M, Maduwuba M C, In Silico Docking Analysis of Anti-malaria and Anti-typhoid Potentials of Phytochemical Constituents of Ethanol Extract of Dryopteris dilatata, Tropical Journal of Natural Product Research. 2022, 6 (5):772-782.
20. Adindu C B, In-Silico Screening of Lung Cancer Inhibiting Potential of the Chemical Constituents of N-Hexane Extract of Elaisi guineenses, Journal of Materials Science Research and Reviews, 2023, 6(3): 572-582.
21. Arthur M N, Bebla K, Broni E, Ashley C, Velazquez M, Hua X, Radhakrishnan R, Kwofie S K, Miller WA, Design of Inhibitors That Target the Menin–Mixed-Lineage Leukemia Interaction. Computation. 2024, 12(1) 3. https://doi.org/10.3390/computation12010003
22. Singh A N, Baruah M M, Sharma N. Structure Based docking studies towards exploring potential anti-androgen activity of selected phytochemicals against Prostate Cancer. Scientific Reports. 2017, 16:7(1) :1955. doi: 10.1038/s41598-017-02023-5. PMID: 28512306; PMCID: PMC5434041.
23. Pedro M M, et al, Structural Evidence for Ligand Specificity in the Binding Domain of the Human Androgen Receptor, implications for pathogenic gene mutations, Journal of biological chemistry, 2000, 275 (34):26164-26171.
24. Sujana D, Sumiwi S A. Saptarini N M, Levita J, Admet prediction and molecular docking simulation of phytoconstituents in Boesenbergia rotunda rhizome with the effector caspases to understand their protective effects, Rasayan journal of Chemistry, 2022, 15 (4) :2401-2406.
25. Tripathi D, Koora S, Satyanarayana K, Saleem Basha S, Jayaraman S. Molecular docking analysis of COX-2 with compounds from Piper longum. Bioinformation. 2021, 17(6) :623-627. doi: 10.6026/97320630017623. PMID: 35173384; PMCID: PMC8819790.
26. Rahul T, Bruce A. R, Makedonka M, In Silico Drug Design, Academic Press. (2019) 329-358, https://doi.org/10.1016/B978-0-12-816125-8.00012-2.
27. Oguzie E E Ogukwe C E Ogbulie J N Nwanebu F C Adindu C B Udeze I O Oguzie K L Eze F C Broad spectrum corrosion inhibition: corrosion and microbial (SRB) growth inhibiting effects of Piper guineense extract, Journal of Material Science. 2012, (47) 3592–360

UNDER PEER REVIEW

28. Hussein R K.; Elkhair, H A O, Ibnaouf K H. Spectral, Structural, Stability Characteristics and Frontier Molecular Orbitals of tri-n-butyl phosphate (tbp) and its Degradation Products: DFT calculations. J. Ovonic Res. 2021,17, 23–30. Available online:
29. A. Rauk, Orbital Interaction Keory of Organic Chemistry p. 86, 2nd edition, Wiley-Interscience, Hoboken, NJ, USA, 2001.

UNDER PEER REVIEW